

# Aberrant controllability of functional connectome during working memory tasks in patients with schizophrenia and unaffected siblings

Feiwen Wang, Zhening Liu, Ju Wang, Xiao Li, Yunzhi Pan, Jun Yang, Peng Cheng, Fuping Sun, Wenjian Tan, Danqing Huang, Jiamei Zhang, Xiawei Liu, Maoxing Zhong, Guowei Wu, Jie Yang and Lena Palaniyappan

## Background

Working memory deficit, a key feature of schizophrenia, is a heritable trait shared with unaffected siblings. It can be attributed to dysregulation in transitions from one brain state to another.

## Aims

Using network control theory, we evaluate if defective brain state transitions underlie working memory deficits in schizophrenia.

## Method

We examined average and modal controllability of the brain's functional connectome in 161 patients with schizophrenia, 37 unaffected siblings and 96 healthy controls during a two-back task. We use one-way analysis of variance to detect the regions with group differences, and correlated aberrant controllability to task performance and clinical characteristics. Regions affected in both unaffected siblings and patients were selected for gene and functional annotation analysis.

## Results

Both average and modal controllability during the two-back task are reduced in patients compared to healthy controls and siblings, indicating a disruption in both proximal and distal state

transitions. Among patients, reduced average controllability was prominent in auditory, visual and sensorimotor networks. Reduced modal controllability was prominent in default mode, frontoparietal and salience networks. Lower modal controllability in the affected networks correlated with worse task performance and higher antipsychotic dose in schizophrenia (uncorrected). Both siblings and patients had reduced average controllability in the paracentral lobule and Rolandic operculum. Subsequent out-of-sample gene analysis revealed that these two regions had preferential expression of genes relevant to bioenergetic pathways (calmodulin binding and insulin secretion).

## Conclusions

Aberrant control of brain state transitions during task execution marks working memory deficits in patients and their siblings.

## Keywords

Cognitive deficits; dynamic; psychosis; connectivity; genetic risk.

## Copyright and usage

© The Author(s), 2025. Published by Cambridge University Press on behalf of Royal College of Psychiatrists.

Working memory is a foundational component of information processing and problem-solving.<sup>1</sup> Working memory deficit is a key feature of schizophrenia, which emerges before the onset of illness and persists even after symptomatic remission, leading to a lifelong cognitive burden. Considerable evidence points to working memory deficit being an important endophenotype seen in both patients with schizophrenia and their unaffected siblings who share their genetic liability.<sup>2,3</sup> Unlike patients, siblings are free from the influence of antipsychotics and chronic disease course. Therefore, studying unaffected siblings reduces the treatment and illness confounds when investigating the genetically mediated pathophysiology of working memory deficits.

## Brain state transitions

When executing a working memory task, systematic transition through various global brain states (i.e. stable or quasi-stable, condition-dependent organisation of whole-brain connectivity profile/patterns that support adaptive functions)<sup>4</sup> along with an adaptable reconfiguration of brain-wide interactions appear to be necessary.<sup>5-7</sup> Evidence indicates that patients with schizophrenia exhibit notable alteration in this working memory-related reconfiguration. When performing working memory tasks, patients often exhibit an inefficient topological arrangement within the comprehensive brain connectome. This inefficiency manifests as heightened segregation among brain networks, accompanied by a shift in the distribution of network degrees towards a more uniform pattern of connectivity.<sup>8</sup> When working memory-related dynamic (time-varying) brain network characteristics are considered, patients exhibit unstable activity,<sup>9</sup> disrupted connectivity<sup>10</sup> and

inappropriately heightened network flexibility.<sup>11</sup> The heightened network flexibility is also seen in unaffected relatives, albeit to a lesser extent than in patients with schizophrenia, potentially representing a network-based intermediate phenotype associated with genetic susceptibility to schizophrenia.<sup>11</sup> We can obtain novel insights into the genetically mediated failure modes in the dynamic working memory system by studying functional network reconfigurations during task performance in patients and siblings.

## Application of control theory

Classical control theory offers a mathematical framework for understanding how the brain's connectivity changes over time.<sup>12</sup> Its principles, originating from engineering, suggest that the brain transitions between different functional states or operating modes in response to energy input; this enhances the system's functionality in response to demands.<sup>12,13</sup> By analysing functional magnetic resonance imaging (fMRI) data, we can identify these different brain states and how the brain's network structure enables transitions between them.

*Average controllability* and *modal controllability* stand out as the most frequently utilised indicators of controllability.<sup>12</sup> Average controllability signifies the reciprocal of the average pulse response energy (control input) required to facilitate the brain's transition to easily attainable states.<sup>14</sup> Nodes exhibiting higher average controllability demand less energy to change from their current state, thereby indicating excellent flexibility in manoeuvring their operating mode in the ongoing brain state.<sup>12,15</sup> Conversely, modal controllability serves to evaluate the nodes' capacity to transition to demanding brain states. Regions with higher modal controllability

are positioned to drive the dynamics of a brain network towards hard-to-reach states, which imposes low energy costs for completing complex goal-specific operations.<sup>12</sup>

Previous fMRI work in healthy individuals indicates that during working memory tasks, several nodes within the salience network exhibited the highest average controllability across the entire brain.<sup>15</sup> Meanwhile, the average controllability of the salience network, frontoparietal network (FPN) and default mode network (DMN; i.e. triple network) decreased with the escalation of the task load<sup>15</sup> (i.e. more input signals are required to enable transition). First-episode never-treated patients with schizophrenia show higher average controllability and lower modal controllability in the dorsal anterior cingulate cortex compared to healthy controls at the resting state.<sup>12</sup> However, the control characteristics of the functional connectome during working memory tasks are bound to differ from those in the resting state; this has not yet been studied in schizophrenia. We also do not know whether the disrupted brain controllability would be observed in unaffected siblings and thus influenced by the genetic predisposition related to schizophrenia.

## Objectives

The objective of this study was to characterise the functional network controllability during working memory tasks in patients with schizophrenia and unaffected, genetically related siblings. We employed the tools of the control theory and investigated the brain controllability across the brain in patients, their siblings and matched healthy controls.<sup>16</sup> We tested whether the degree of controllability of regions showing inter-group differences varied with the observed working memory performance and individual clinical characteristics. We also conducted an out-of-sample imaging transcriptomic analysis to explore the genetic relevance of regional aberrations in brain controllability that are shared between patients and their siblings.<sup>17</sup>

## Method

### Participants

The study cohort comprised 172 patients with schizophrenia, 43 unaffected siblings and 102 healthy controls. All participants were right-handed native Chinese speakers and signed written informed consent to participate in this study. The authors assert that all procedures contributing to this work comply with the ethical standards of the relevant national and institutional committees on human experimentation and with the Helsinki Declaration of 1975, as revised in 2013. All procedures involving human participants were approved by the medical ethics committee of the Second Xiangya Hospital, Central South University, reference (2021) National Review (Science and Technology) No. (015). Detailed information for recruitment is provided in Supplementary Material 1, available at <https://doi.org/10.1192/bjp.2024.225>.

### Magnetic resonance imaging data acquisition and preprocessing

Magnetic resonance imaging (MRI) data were acquired using a Siemens Allera 3-T scanner. A working memory paradigm was implemented in the scanner. Detailed scanning parameters and preprocessing procedure are provided in Supplementary Material 2.

There were 11 patients with schizophrenia, six unaffected siblings and six healthy controls excluded owing to large head motion and failures in the normalisation and registration to Montreal Neurological Institute space. The final analysis cohort comprised 161 patients with schizophrenia, 37 unaffected siblings and 96 healthy controls. No significant differences were observed in the overall count of interpolated displaced volumes among all groups

(mean  $\pm$  s.d.: patients with schizophrenia  $10.9 \pm 15.2$ , unaffected siblings  $9.9 \pm 13.7$ , healthy controls  $10.1 \pm 14.1$ ,  $P = 0.661$ ).

### Working memory task paradigm

We adopted the  $n$ -back task as the working memory paradigm, and the 'zero-back' and 'two-back' loads were applied in our research. A detailed description of this paradigm is given in Supplementary Material 3 and Supplementary Fig. 1.

### Controllability calculation

Before calculating the average and modal controllability, we reorganised the preprocessed fMRI data. For each participant, we separately concatenated the fMRI volumes obtained under the four blocks of the 'zero-back' load and the four blocks of the 'two-back' load, and we generated these two loads of fMRI data with 80 volumes each. We extracted the mean time series from each of the 264 nodes using 6 mm spheres defined by the Power atlas,<sup>18</sup> and generated a  $264 \times 264$  symmetric matrix for each participant by computing the Pearson correlation coefficients between the time series for each pair of regions of interest (ROIs). The resultant matrix was converted to normally distributed scores by using Fisher's  $z$  transformation.

Then, we computed the average and modal controllability in the matrix that was constructed on 'zero-back' and 'two-back' loads, separately. Calculation of controllability was based on prior neuroimaging studies and employed control theory notations.<sup>12</sup> Network controllability reflects the ability of external control energy to drive the current network state to other desired target states (see Fig. 2). *Average controllability* measures the ability of a node to drive the brain to all possible easy-to-reach configurations by considering the average input energy cost. Higher average controllability of a node indicates a more crucial role in enabling transitions of the network system between states. *Modal controllability* mathematically evaluates the ability of a node to control all the dynamic modes of the network. Higher modal controllability of a node indicates a stronger ability to drive the dynamics towards hard-to-reach configurations. Details of the computation of these metrics are provided in Supplementary Material 4.

### Statistical analysis

We utilised SPSS statistical software (version 22 for Windows) to compare demographic and clinical characteristics as well as working memory task performance across groups. Differences in age, years of education, accuracy and response time under the 'zero-back' and 'two-back' loads were analysed using one-way analysis of variance (ANOVA) tests. Gender differences were assessed using  $\chi^2$  tests.

For the statistical analysis of controllability metrics, we employed MATLAB 2018 software for Windows (Mathworks, Natick, Massachusetts, USA; <https://www.mathworks.com/>). Controllability data for each participant were subjected to group analysis using the one-way ANOVA test to examine group differences. Gender, age, years of education and head motion parameters were included as covariates in the analysis of controllability metrics to account for potential confounding factors. We corrected all data for multiple comparisons using false discovery rate (FDR) correction at  $P < 0.05$ . Then, *post hoc* tests were performed between each two-group pair using a threshold at  $P < 0.05$  with Tukey correction to examine the distinction of the controllability among patients with schizophrenia, unaffected siblings and healthy controls groups respectively.

We performed correlation analyses to investigate whether the regionally altered controllability (i.e. excluding the effects of gender, age, years of education and head motion parameters) correlated with cognitive performance (including  $n$ -back task

performance, Wechsler Adult Intelligence Scale (WAIS) information, and WAIS digit symbol subscales) or clinical characteristics (scores of Scale for Assessment of Positive Symptoms (SAPS), Scale for Assessment of Negative Symptoms (SANS), illness duration and antipsychotic dosage) in schizophrenia.

### Exploratory analysis

We further conducted an imaging transcriptomic analysis estimating the spatial correlation between the regions with shared changes between patients with schizophrenia and unaffected siblings and an established gene expression atlas. These ROIs were defined as the regions in which both the patients with schizophrenia and unaffected siblings showed significant controllability difference (*post hoc t-test* ( $P$ -Tukey < 0.05) after *F-test* ( $P$ -fdr < 0.05)) compared to healthy controls, in the same direction (i.e. the controllability in both groups was higher or lower than that of healthy controls).

#### Imaging transcriptomic analysis

We used the Brain Annotation Toolbox (BAT; version 1.1 for Windows, Institute of Science and Technology for Brain-Inspired Intelligence, Fudan University, Shanghai, China; <http://istbi.fudan.edu.cn/bat/index.html>) to perform genetic and functional annotation analysis on the selected regions.<sup>19</sup> BAT was employed to extract functional information from Neurosynth and gene expression profiles from the Allen Human Brain Atlas (AHBA). This process was based on brain regions defined by clusters of voxels. The permutation

analysis was performed 5000 times to ensure robustness. Other parameters for genetic and functional annotations included a ROI size set at 6 mm and a minimal sample size of five. These parameters were chosen to optimise the functional and genetic annotation process and enhance the reliability of the results.

#### Enrichment analysis

The derived differentially expressed genes were uploaded to the Database for Annotation, Visualization, and Integrated Discovery (DAVID) (<https://david.ncifcrf.gov/>). Gene Ontology database analysis was conducted, specifically focusing on three domains: the biological process, cellular component and molecular function. In addition, the Kyoto Encyclopedia of Genes and Genomes (KEGG) database for *Homo sapiens* sets was utilised for gene function and pathway enrichment analysis. To determine statistical significance, the threshold for significance was set at a FDR-adjusted  $P$ -value of less than 0.05. This approach controlled type-1 error from multiple tests and ensured that the identified gene functions and pathways were less likely to be false positives.

## Results

### Participants characteristics

Demographic and clinical findings of this study cohort are presented in Table 1. Patients with schizophrenia were younger than unaffected siblings ( $P < 0.001$ ) and healthy controls ( $P < 0.001$ ).

**Table 1** Demographic, clinical and neurocognitive information

Variables	Patients with schizophrenia (N = 161)	Unaffected siblings (N = 37)	Healthy controls (N = 96)	F/t/ $\chi^2$	P	Post hoc Tukey significance
Age (years)	17.91 ± 3.26	21.94 ± 6.19	20.69 ± 3.67	26.011	<0.001*	Healthy controls > patients with schizophrenia: $P < 0.001$ ; unaffected siblings > patients with schizophrenia: $P < 0.001$
Gender (M/F)	84/77	13/24	49/47	3.603	0.165	N/A
Education (years)	10.62 ± 2.32	11.83 ± 3.05	13.18 ± 3.16	28.161	<0.001*	Healthy controls > unaffected siblings: $P = 0.030$ ; healthy controls > patients with schizophrenia: $P < 0.001$ ; unaffected siblings > patients with schizophrenia: $P = 0.042$
SAPS score	26.18 ± 19.02	N/A	N/A	N/A	N/A	N/A
SANS score	37.95 ± 28.63	N/A	N/A	N/A	N/A	N/A
Total dosage (mg/d) <sup>a</sup>	425 ± 270	N/A	N/A	N/A	N/A	N/A
Illness duration (months)	20.35 ± 23.13	N/A	N/A	N/A	N/A	N/A
WAIS-CR information	15.31 ± 6.09	16.07 ± 5.41	19.07 ± 5.43	13.514	<0.001*	Healthy controls > unaffected siblings: $P = 0.023$ ; healthy controls > patients with schizophrenia: $P < 0.001$
WAIS-CR digit symbol	62.00 ± 17.90	84.14 ± 15.12	88.21 ± 17.12	79.059	<0.001*	Healthy controls > patients with schizophrenia: $P < 0.001$ ; unaffected siblings > patients with schizophrenia: $P < 0.001$
ACC of zero-back load (%)	81 ± 22	90 ± 22	95 ± 9	15.062	<0.001*	Healthy controls > patients with schizophrenia: $P < 0.001$ ; unaffected siblings > patients with schizophrenia: $P = 0.031$
Response time of zero-back load (ms)	554 ± 135	514 ± 69	494 ± 75	9.009	<0.001*	Healthy controls < patients with schizophrenia: $P < 0.001$
ACC of two-back load (%)	61 ± 44	74 ± 22	79 ± 18	8.659	<0.001*	Healthy controls > patients with schizophrenia: $P < 0.001$
Response time of two-back load (ms)	725 ± 197	689 ± 159	661 ± 138	3.930	0.021*	Healthy controls < patients with schizophrenia: $P = 0.016$

N/A, not applicable; SAPS, Scale for Assessment of Positive Symptoms; SANS, Scale for Assessment of Negative Symptoms; WAIS-CR, Wechsler Adult Intelligence Scale-Chinese Revised; ACC, accuracy.  
<sup>a</sup> Antipsychotic dosage refers to dose equivalents for chlorpromazine calculated using the classical mean dose method.<sup>20</sup>  
 \*  $P < 0.05$ .

Besides, there was a 'ladder' pattern of education years among the three groups ( $F = 28.161$ ,  $P < 0.001$ ; healthy controls > unaffected siblings:  $P = 0.030$ ; healthy controls > patients with schizophrenia:  $P < 0.001$ ; unaffected siblings > patients with schizophrenia:  $P = 0.042$ ). In terms of working memory task performance, the healthy controls performed better than the patients with schizophrenia at both the 'zero-back' ( $P < 0.001$ ) and 'two-back' ( $P < 0.001$ ) loads. The difference between the siblings and the other two groups was not significant for the two-back load. For the 'zero-back' load, unaffected siblings performed better than the patients with schizophrenia ( $P = 0.031$ ). Detailed information is presented in Table 1.

### Controllability metrics

#### Average controllability

Under 'zero-back' load, one-way ANOVA revealed a significant omnibus difference of average controllability across all diagnostic groups in the visual network (node numbers 2) and ventral attention network (VAN, node numbers 1) (see Supplementary Table 1 and Supplementary Fig. 3); under 'two-back' load, one-way ANOVA revealed a significant omnibus difference of average controllability across all diagnostic groups in the sensorimotor network (SMN, node numbers 2), auditory network (node numbers 2), visual network (node numbers 2) and memory retrieval network (MRN, node numbers 1) (see Table 2 and Fig. 1).

#### Modal controllability

Under 'zero-back' load, one-way ANOVA revealed a significant omnibus difference of modal controllability across all diagnostic groups in the DMN (node numbers 2) and FPN (node numbers 1) (see Supplementary Table 1 and Supplementary Fig. 4); Under 'two-back' load, one-way ANOVA revealed a significant omnibus difference of modal controllability across all diagnostic groups in the DMN (node numbers 24), FPN (node numbers 13), salience network (node numbers 9), cingulo-opercular network (CON, node numbers 1) and dorsal attention network (DAN, node numbers 2) (see Table 2 and Fig. 1).

Interestingly, patients with schizophrenia exhibited lower average and modal controllability in all detected regions compared to healthy controls and unaffected siblings. Unaffected siblings generally exhibited increased controllability compared with healthy controls in most detected regions. Under 'two-back' load, compared with healthy controls, patients with schizophrenia and unaffected siblings both showed lower average controllability in the right-hand paracentral lobule ( $P\text{-}fdr = 0.035$ ) and the right-hand Rolandic operculum ( $P\text{-}fdr = 0.035$ ). Details are shown in Table 2 and Fig. 2. To examine the influence of gender and antipsychotic dose, we also conducted a stratified analysis and observed no significant differences in controllability between genders or dose-based subgroups in patients (see Supplementary Tables 2–5).

In the Pearson correlation analysis, the average controllability during both 'zero-back' and 'two-back' loads showed poor correlation with cognitive performance and clinical characteristics among patients. However, higher modal controllability in some of the affected regions ('zero-back': two nodes in the DMN; 'two-back': 13 nodes in the DMN, five nodes in the salience network and one node in the FPN) was seen in association with better performance of the corresponding task load. Besides, higher modal controllability of certain regions ('zero-back': one node in the DMN and one node in the FPN; 'two-back': five nodes in the FPN, two nodes in the DMN and two nodes in the salience network) was associated with lower prescribed antipsychotic dose. In two DMN regions, modal controllability was negatively

correlated with the scores of SANS ('two-back'). We also performed the correlation analysis in unaffected siblings and healthy controls. Unaffected siblings shared a similar correlation relationship between working memory performance and modal controllability in several nodes (one node in the DMN and one node in the FPN) under 'two-back' load. Detailed information is shown in Supplementary Tables 6–13, and Figs. 5 and 6. However, no significant correlation relationship survives FDR correction.

### Exploratory analysis

The right-hand paracentral lobule and right-hand Rolandic operculum both showed shared changes in controllability in both patients with schizophrenia and unaffected siblings; imaging transcriptomic analysis was focused on these ROIs.

The functional annotation analyses identified nine functional labels consistently related to the regions showing aberrant average controllability – nociceptive, pain, sensation, multisensory, touch, pressure, somatosensory, primary somatosensory and secondary somatosensory functions (see Fig. 2). However, no significant results were observed after FDR correction.

The genetic annotation analyses identified 36 genes with spatially relative overexpression for regions with aberrant average controllability ( $P\text{-}fdr < 0.05$ ). For the Gene Ontology enrichment analysis, in terms of the molecular function, calmodulin binding ( $P\text{-}fdr = 0.015$ , RGS4, NOS2, ADCY1, CAMK2G, KCNH1) represented statistically significant enrichment. In terms of the KEGG pathway, insulin secretion ( $P\text{-}fdr = 0.014$ , ADCY1, ATP1A1, CAMK2G) represented statistically significant enrichment (see Fig. 2). No prominent enrichment was observed in terms of biological processes and cellular components. Detailed information on genetic annotation analysis is provided in Supplementary Tables 14 and 15. We also performed *post hoc* enrichment analysis for regions with altered controllability in patients but not in siblings (compared to healthy controls) to gain insights into illness-specific biological mechanisms; the significantly enriched gene expression abnormalities identified in the gene enrichment analysis are predominantly associated with synaptic functions (see Supplementary Material 5 and Supplementary Fig. 7).

## Discussion

We report four novel findings on the controllability of the functional connectome during a working memory task in patients with schizophrenia, unaffected siblings and healthy controls. First, controllability differs between groups during task performance, especially when there is higher working memory demand (two-back). Patients show reduced average controllability compared with healthy controls and siblings, especially in the unimodal sensory networks (visual network, auditory network and SMN). This indicates reduced flexibility in shifting to task-free (relatively easy-to-reach) brain states. Second, lower modal controllability in patients is predominantly seen in the triple network regions of the default mode, frontoparietal and salience network, indicating that these regions require more 'energy' (in the sense of external inputs) to reach the relatively demanding states needed for complex cognitive operations. Third, at an uncorrected threshold, lower modal controllability relates to poor working memory task performance in some regions and higher dose of antipsychotics in other regions. Fourth, unaffected siblings had preserved controllability metrics that were numerically higher than healthy controls across most brain regions. Nonetheless, like patients, they also had reduced controllability in the paracentral lobule and Rolandic operculum when compared to healthy controls. Spatial



**Table 2** Controllability difference across patients with schizophrenia, unaffected siblings and healthy controls at the 'two-back' load

ROI No.	Network	Brain region	MNI space			FDR-corrected <i>P</i>	Post hoc Tukey significance			Mean (controllability)		
			<i>x</i>	<i>y</i>	<i>z</i>		Healthy controls versus unaffected siblings	Healthy controls versus patients with schizophrenia	Unaffected siblings versus patients with schizophrenia	Healthy controls	Unaffected siblings	Patients with schizophrenia
Average controllability												
25	SMN	R_Postcentral gyrus	29	-39	59	<0.001*	0.678	<0.001*	0.001*	0.0194	0.0321	-0.0190
39#	SMN	R_Paracentral lobule	2	-28	60	<0.001*	0.035*	<0.001*	0.697	0.0313	-0.0059	-0.0173
63	Auditory network	R_Superior temporal gyrus	58	-16	7	<0.001*	0.217	<0.001*	0.187	0.0329	0.0058	-0.0209
71#	Auditory network	R_Rolandic operculum	56	-5	13	<0.001*	0.040*	<0.001*	0.244	0.0347	0.0005	-0.0208
151	Visual network	L_Lingual gyrus	-15	-72	-8	<0.001*	0.537	0.001*	0.001*	0.0178	0.0341	-0.0185
161	Visual network	R_Inferior temporal gyrus	42	-66	-8	<0.001*	0.009*	0.015*	<0.001*	0.0096	0.0534	-0.0180
136	MRN	R_Precuneus	4	-48	51	<0.001*	0.461	<0.001*	<0.001*	0.0216	0.0421	-0.0226
254	Uncertain	R_Middle temporal gyrus	46	-47	-17	<0.001*	0.028*	0.033*	<0.001*	0.0077	0.0411	-0.0140
Modal controllability												
79	DMN	L_Middle temporal gyrus	-46	-61	21	<0.001*	0.696	<0.001*	0.001*	0.0007	0.0011	-0.0007
83	DMN	L_Middle temporal gyrus	-68	-23	-16	<0.001*	0.991	<0.001*	0.013*	0.0008	0.0008	-0.0007
86	DMN	L_Angular gyrus	-44	-65	35	<0.001*	0.633	<0.001*	<0.001*	0.0010	0.0015	-0.0009
87	DMN	L_Precuneus	-39	-75	44	<0.001*	0.647	<0.001*	0.001*	0.0009	0.0014	-0.0008
96	DMN	R_Angular gyrus	52	-59	36	<0.001*	0.513	<0.001*	<0.001*	0.0010	0.0017	-0.0010
97	DMN	R_Superior frontal gyrus	23	33	48	<0.001*	0.619	0.001*	0.001*	0.0007	0.0013	-0.0007
98	DMN	L_Medial frontal gyrus	-10	39	52	<0.001*	0.464	0.001*	<0.001*	0.0007	0.0015	-0.0008
99	DMN	L_Superior frontal gyrus	-16	29	53	<0.001*	0.688	<0.001*	0.001*	0.0008	0.0014	-0.0008
101	DMN	R_Superior frontal gyrus	22	39	39	<0.001*	0.392	<0.001*	<0.001*	0.0007	0.0014	-0.0008
102	DMN	R_Medial frontal gyrus	13	55	38	<0.001*	0.131	<0.001*	<0.001*	0.0007	0.0018	-0.0008
104	DMN	L_Superior frontal gyrus	-20	45	39	<0.001*	0.921	<0.001*	0.004*	0.0008	0.0010	-0.0007
105	DMN	R_Medial frontal gyrus	6	54	16	<0.001*	0.274	0.001*	<0.001*	0.0007	0.0017	-0.0008
108	DMN	R_Medial frontal gyrus	9	54	3	<0.001*	0.834	<0.001*	0.002*	0.0008	0.0012	-0.0008
112	DMN	L_Medial frontal gyrus	-2	38	36	<0.001*	0.640	<0.001*	<0.001*	0.0010	0.0016	-0.0010
113	DMN	L_Anterior cingulate gyrus	-3	42	16	<0.001*	0.233	0.004*	<0.001*	0.0006	0.0015	-0.0007
114	DMN	L_Superior frontal gyrus	-20	64	19	<0.001*	0.430	<0.001*	<0.001*	0.0007	0.0014	-0.0008
115	DMN	L_Medial frontal gyrus	-8	48	23	<0.001*	0.228	0.001*	<0.001*	0.0007	0.0017	-0.0008
119	DMN	R_Middle temporal gyrus	65	-31	-9	<0.001*	0.906	<0.001*	<0.001*	0.0009	0.0011	-0.0008
121	DMN	R_Medial frontal gyrus	13	30	59	<0.001*	0.630	<0.001*	<0.001*	0.0008	0.0013	-0.0008
127	DMN	Cerebellum_Crus1_R	28	-77	-32	<0.001*	0.957	<0.001*	0.002*	0.0008	0.0009	-0.0007
128	DMN	R_Middle temporal gyrus	52	7	-30	<0.001*	0.606	0.001*	0.001*	0.0006	0.0011	-0.0006
130	DMN	R_Angular gyrus	47	-50	29	<0.001*	0.277	<0.001*	<0.001*	0.0008	0.0017	-0.0008
137	DMN	L_Inferior frontal gyrus	-46	31	-13	<0.001*	0.912	<0.001*	0.001*	0.0012	0.0009	-0.0009
139	DMN	R_Inferior frontal gyrus	49	35	-12	<0.001*	0.832	<0.001*	0.001*	0.0007	0.0010	-0.0007
177	FPN	L_Inferior parietal gyrus	-53	-49	43	<0.001*	0.998	<0.001*	0.003*	0.0009	0.0010	-0.0008
178	FPN	L_Superior frontal gyrus	-23	11	64	<0.001*	0.977	<0.001*	0.003*	0.0009	0.0010	-0.0008
181	FPN	R_Middle orbital frontal gyrus	34	54	-13	<0.001*	0.307	<0.001*	<0.001*	0.0008	0.0017	-0.0009
190	FPN	R_Inferior parietal gyrus	49	-42	45	<0.001*	0.394	<0.001*	<0.001*	0.0010	0.0019	-0.0010
192	FPN	R_Inferior parietal gyrus	44	-53	47	<0.001*	0.318	<0.001*	<0.001*	0.0009	0.0019	-0.0010
193	FPN	R_Middle frontal gyrus	32	14	56	<0.001*	0.307	0.001*	<0.001*	0.0008	0.0018	-0.0009
194	FPN	R_Angular gyrus	37	-65	40	<0.001*	0.240	<0.001*	<0.001*	0.0007	0.0016	-0.0008
195	FPN	L_Inferior parietal gyrus	-42	-55	45	<0.001*	0.699	<0.001*	<0.001*	0.0010	0.0015	-0.0009
196	FPN	R_Middle frontal gyrus	40	18	40	<0.001*	0.397	<0.001*	<0.001*	0.0008	0.0015	-0.0008

(Continued)

Table 2 (Continued)

ROI No.	Network	Brain region	MNI space			FDR-corrected <i>P</i>	Post hoc Tukey significance			Mean (controllability)		
			<i>x</i>	<i>y</i>	<i>z</i>		Healthy controls versus unaffected siblings	Healthy controls versus patients with schizophrenia	Unaffected siblings versus patients with schizophrenia	Healthy controls	Unaffected siblings	Patients with schizophrenia
197	FPN	L_Middle frontal gyrus	-34	55	4	<0.001*	0.100	<0.001*	<0.001*	0.0007	0.0019	-0.0009
198	FPN	L_Middle orbital frontal gyrus	-42	45	-2	<0.001*	0.551	<0.001*	<0.001*	0.0008	0.0015	-0.0008
199	FPN	R_Inferior parietal gyrus	33	-53	44	<0.001*	0.655	<0.001*	0.001*	0.0008	0.0013	-0.0008
200	FPN	R_Middle orbital frontal gyrus	43	49	-2	<0.001*	0.169	<0.001*	<0.001*	0.0007	0.0018	-0.0008
204	Saliency network	R_Supramarginal gyrus	55	-45	37	<0.001*	0.597	<0.001*	<0.001*	0.0008	0.0014	-0.0008
207	Saliency network	R_Inferior frontal gyrus, triangular part	48	22	10	<0.001*	0.349	<0.001*	<0.001*	0.0006	0.0013	-0.0006
213	Saliency network	L_Supplementary motor area	-1	15	44	<0.001*	0.429	<0.001*	<0.001*	0.0008	0.0017	-0.0009
214	Saliency network	L_Middle frontal gyrus	-28	52	21	<0.001*	0.154	<0.001*	<0.001*	0.0007	0.0017	-0.0008
215	Saliency network	L_Anterior cingulate gyrus	0	30	27	<0.001*	0.366	<0.001*	<0.001*	0.0007	0.0014	-0.0007
216	Saliency network	R_Middle cingulate gyrus	5	23	37	<0.001*	0.527	<0.001*	<0.001*	0.0008	0.0014	-0.0008
218	Saliency network	R_Superior frontal gyrus	31	56	14	<0.001*	0.112	<0.001*	<0.001*	0.0008	0.0019	-0.0009
219	Saliency network	R_Middle frontal gyrus	26	50	27	<0.001*	0.074	0.001*	<0.001*	0.0006	0.0017	-0.0007
220	Saliency network	L_Middle frontal gyrus	-39	51	17	<0.001*	0.373	<0.001*	<0.001*	0.0007	0.0015	-0.0008
50	CON	L_Superior frontal gyrus	-16	-5	71	<0.001*	0.428	<0.001*	<0.001*	0.0008	0.0015	-0.0008
259	DAN	L_Inferior parietal gyrus	-33	-46	47	<0.001*	0.374	0.001*	<0.001*	0.0007	0.0015	-0.0007
264	DAN	R_Paracental lobule	29	-5	54	<0.001*	0.994	<0.001*	0.005*	0.0008	0.0009	-0.0007
9	Uncertain	R_Middle temporal gyrus	65	-24	-19	<0.001*	0.943	<0.001*	0.003*	0.0007	0.0009	-0.0006
11	Uncertain	R_Inferior temporal gyrus	55	-31	-17	<0.001*	0.178	0.001*	<0.001*	0.0005	0.0013	-0.0006
84	Uncertain	L_Middle temporal gyrus	-58	-26	-15	<0.001*	0.995	<0.001*	<0.001*	0.0012	0.0011	-0.0010
184	Uncertain	Cerebellum_Crus2_R	17	-80	-34	<0.001*	0.877	<0.001*	0.003*	0.0010	0.0007	-0.0007
185	Uncertain	Cerebellum_Crus1_R	35	-67	-34	<0.001*	0.855	<0.001*	0.001*	0.0006	0.0009	-0.0006

ROI No., index number of the node in the Power Atlas;<sup>18</sup> MNI, Montreal Neurological Institute; SMN, sensory/somatomotor network; MRN, memory retrieval network; DMN, default mode network; FPN, frontoparietal task control network; CON, cingulo-opercular task control network; DAN, dorsal attention network; ROI, region of interest; FDR, false discovery rate; L, left; R, right.  
\* *P* < 0.05. The controllability values mentioned above are all the residual values of the de-covariant variables.

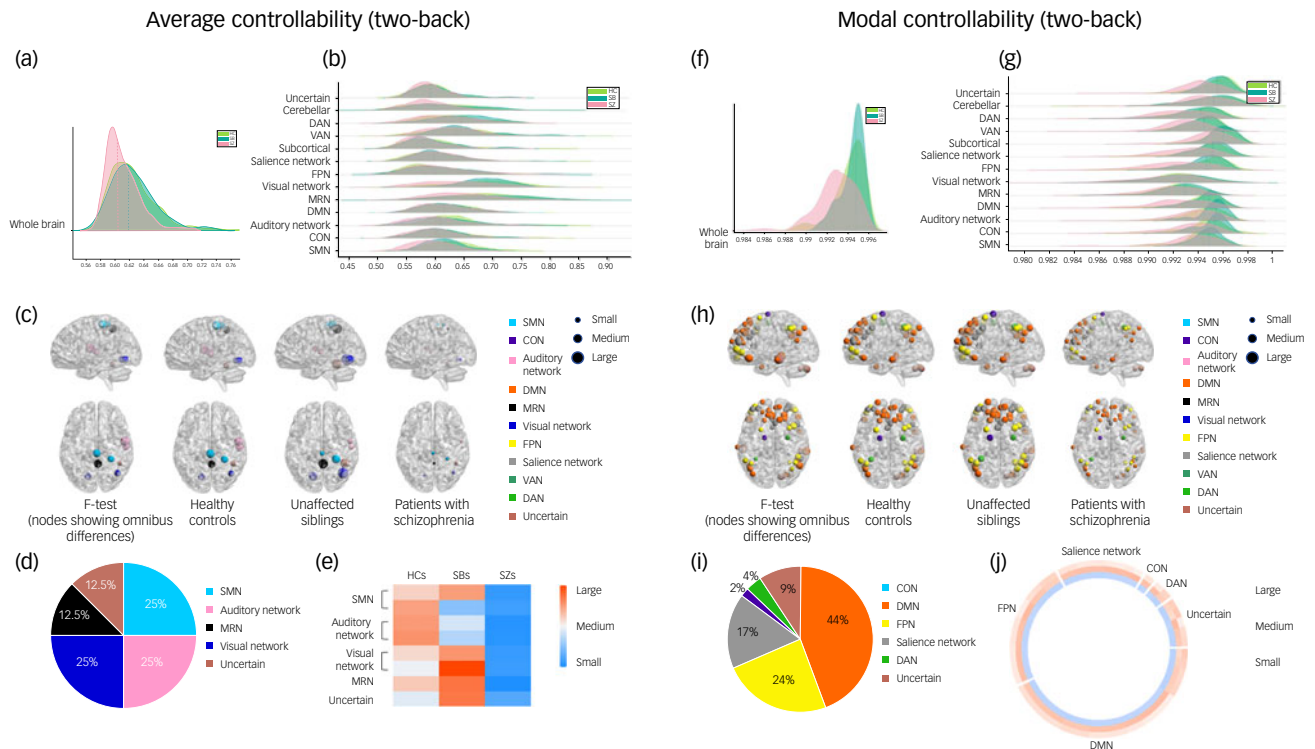


**Fig. 1** Brain regions with group differences in average and modal controllability across all groups under 'two-back' load (omnibus test): (a), (f) distribution of whole-brain controllability; (b), (g) distribution of each large-scale brain network controllability; (c), (h) brain regions showed significantly different controllability across all groups; (d), (i) proportion of detected nodes in each large-scale network; (e), (j) heat map of average controllability and circle heat map of modal controllability each node across all groups. DAN, dorsal attention network; VAN, ventral attention network; FPN, frontoparietal network; MRN, memory retrieval network; DMN, default mode network; CON, cingulo-opercular network; SMN, sensory/somatomotor network; HCs healthy controls; SBs, unaffected siblings; SZs, patients with schizophrenia.

correspondence of gene expression revealed associations with calmodulin binding and insulin secretion pathways. Taken together, these observations provide a nuanced mechanistic framework for working memory deficits in schizophrenia.

We observed large scale inter-group differences in controllability across patients with schizophrenia and unaffected siblings versus healthy controls during two-back tasks. Compared to healthy controls, patients with schizophrenia exhibited a decline in controllability (both modal controllability and average controllability) at all identified regions. Our finding suggests that when manipulating items in working memory, patients with schizophrenia may have a poorer ability to control brain state transitions compared to healthy controls, giving rise to performance deficits that increase with demand. In contrast, unaffected siblings demonstrated an insignificant tendency for increased controllability in the majority of regions compared to healthy controls. Similar distinctive alterations in brain function have been previously reported in studies focused on unaffected siblings and are considered a potential manifestation of resilience/compensation to the disease.<sup>21,22</sup> The inter-group differences in controllability during working memory tasks extended to a broader range of regions with an increased task load. This finding suggests that higher working memory task loads may elicit a greater number of disease-related functional aberrations, aligning with findings from previous research.<sup>23</sup>

When examining the two controllability metrics – modal and average controllability – distinct differences in inter-group brain regions are notable. Modal controllability assesses the capability of brain nodes to transition into states that are relatively challenging to attain, such as cognitively demanding states.<sup>12</sup> The involvement of the triple network system – the DMN, FPN and salience

network – in reduced modal controllability among patients is consistent with its critical role in the execution of working memory and its proposed involvement in the working memory deficits of schizophrenia.<sup>24</sup> During the working memory tasks in healthy controls, there is a decrease in functional connectivity within the DMN and an increase in functional connectivity within the FPN, and the salience network serves a modulatory role in the functional connectivity changes within these two networks.<sup>5,25</sup> Compared to healthy controls, patients with schizophrenia fail to suppress DMN activity and show higher DMN–FPN functional connectivity during task execution,<sup>26</sup> which may relate to aberrant signals from the salience network.<sup>27</sup> Our current findings indicate that triple network dysfunction during working memory tasks in patients with schizophrenia may arise from the higher energy requirements to attain the functional states necessary for performing working memory tasks.

Another notable finding is that, in patients with schizophrenia, the modal controllability in selected regions of the DMN and salience network was lower in those with reduced working memory performance, but these correlations were only shared in part with unaffected siblings. Unaffected siblings have the most pronounced controllability values among the three groups; thus, the relationship between controllability and cognitive function might be more complex, possibly involving nonlinear/compensatory factors in this group. Besides, the modal controllability in regions of the FPN was lower in those receiving higher antipsychotic dosage. This implies that either a higher dose of antipsychotics may preferentially reduce the modal controllability of the FPN or lower FPN controllability may result in a clinical profile that eventually gets higher prescription doses of antipsychotics. This is consistent with the prior observations of the impact of antipsychotic medication

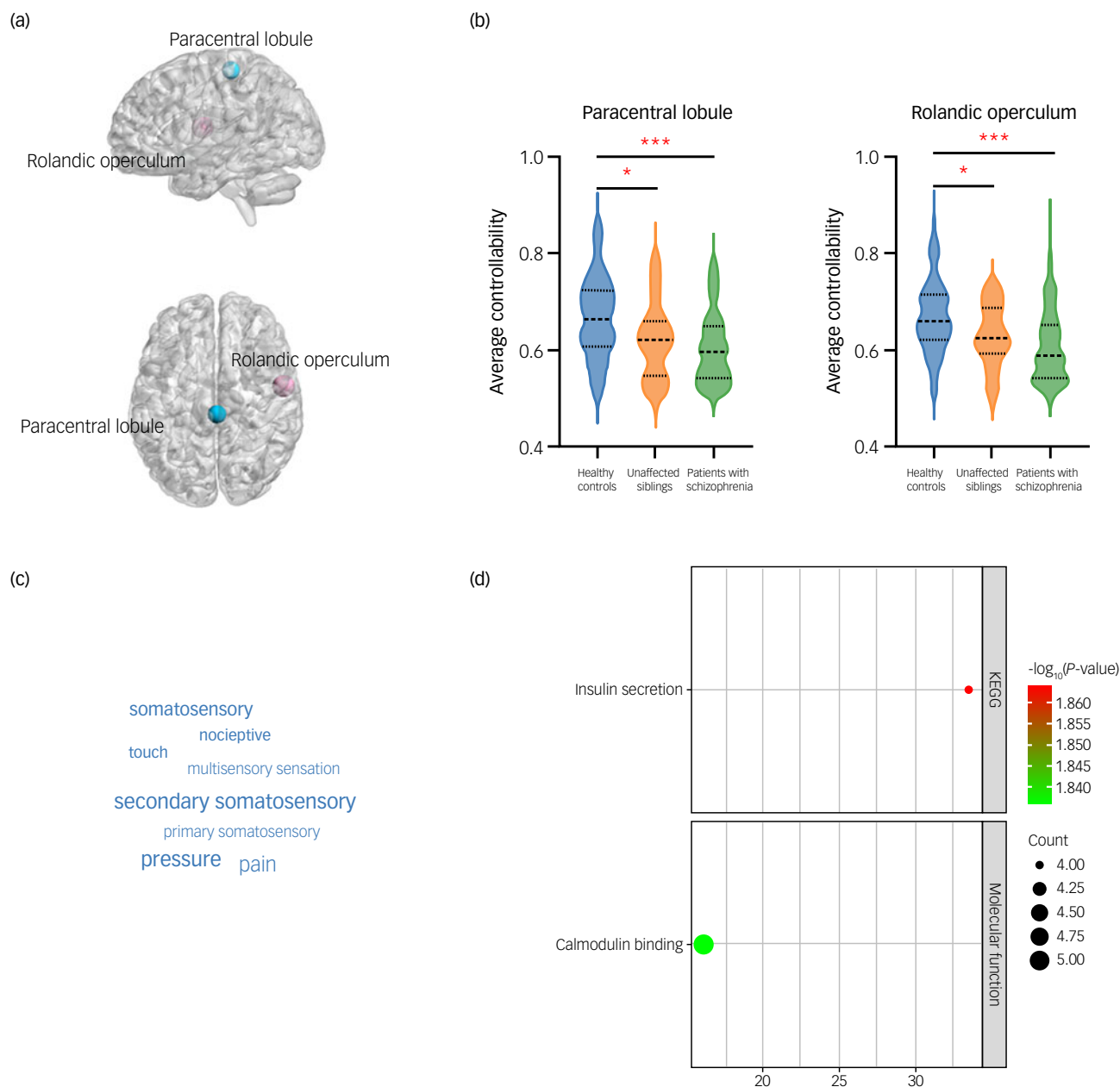


**Fig. 2** Regions where aberrant controllability occurs in both patients with schizophrenia and unaffected siblings, with the results of subsequent genetic and functional analysis: (a) brain nodes that showed common differences in average controllability shared by patients with schizophrenia and unaffected siblings; (b) average controllability gradient across all groups; (c) word cloud map of functional annotation analysis; (d) result of genetic enrichment analysis. KEGG, Kyoto Encyclopedia of Genes and Genomes.

on the activity and functional connectivity of the FPN.<sup>28,29</sup> It is important to note that these results did not survive FDR correction, and a dose-based split group analysis revealed no differential dose effect. But in the absence of data on adherence to treatment and cumulative exposure, we cannot rule out the effect of antipsychotics on FPN controllability. Longitudinal studies that compare the controllability among medicated and unmedicated patients are required for more definitive theories to emerge.

Average controllability evaluates the average capacity to transit into states that are more readily achievable.<sup>12</sup> Disparities in average controllability between groups are predominantly localised in regions associated with primary sensory perception functions, including the auditory network, visual network and SMN, implying a potential deficiency of state transitions in sensory subsystems (compared to transmodal/multimodal regions), especially when

cognitive load is higher. Prior work indicates that during working memory tasks, the visual network and SMN in patients with schizophrenia exhibit distinct temporal profiles of segregation and integration compared with those in healthy controls.<sup>30</sup> The somatosensory cortex not only selectively retains corresponding sensory information temporarily<sup>31</sup> but also demonstrates flexible recruitment by the FPN during task execution to complement the completion of working memory under different sensory patterns.<sup>32</sup> The well-documented sensorimotor and sensory gating impairments in patients with schizophrenia are attributed to their inability to effectively filter out irrelevant external and internal stimuli. This deficiency may result in misperceptions, sensory overload, distractibility and cognitive fragmentation.<sup>33</sup> We have previously reported a link between working memory deficits in schizophrenia and aberrant functional connections in brain regions contributing to the



integration of sensory and motor resources.<sup>34</sup> The findings of this study may contribute new insights into the role of sensorimotor regions in the working memory deficits observed in schizophrenia.


Unaffected siblings and patients with schizophrenia share a decline in controllability in the paracentral lobule and Rolandic operculum compared to healthy controls. This finding suggests a potentially relevant association with the vulnerability observed in unaffected siblings. Grey matter volume (GMV) loss of the paracentral lobule has been reported in patients with schizophrenia and their concordant twin pairs.<sup>35</sup> Interestingly, the operculum showed GMV increase in first-episode schizophrenia and in those at genetically high risk for schizophrenia,<sup>36</sup> but reduced functional connectivity during cognitive tasks in patients with schizophrenia.<sup>10</sup> We note specific gene expression patterns in these affected regions that may be relevant to uncover the bioenergetic pathways contributing to schizophrenia. The gene enrichment analysis suggested that the detected areas are involved in the molecular function of calmodulin binding. Calmodulin was suggested to be a central integrator of synaptic plasticity, and its unique regulatory properties allow the integration of several forms of signal transduction and the regulation of contextual memory.<sup>37</sup> It is important to note that the shared alteration in controllability in patients and siblings does not imply genetic causation, but may result from shared environmental influences as well as gene–environment interactions.

The enrichment of the insulin secretion pathway observed in transcriptomics analysis is relevant to schizophrenia. Insulin plays important roles in neuronal circuitry formation, synaptic maintenance, neuronal survival, dendritic arborisation and learning and memory.<sup>38</sup> While gene enrichment related to insulin secretion has been reported in schizophrenia, it is typically associated with peripheral metabolism<sup>39</sup> with limited insights to date on its impact on the brain function. Besides, we found that the differences between patients with schizophrenia and healthy controls were associated with a gene enrichment and expression pattern related to the synaptic function, which aligns with previous findings linking synaptic dysfunction, neural function and the pathogenesis of schizophrenia.<sup>40</sup>

Our study has some notable limitations. First, we were unable to collect a large sample of age-matched siblings, reducing the variability in this group, although we had sufficient power to demonstrate regional group differences in unaffected siblings versus healthy controls. Second, the effects of medication and the duration of illness cannot be disentangled from the severity of illness *per se* in schizophrenia. As antipsychotic medication was used only in the patients with schizophrenia, we were unable to eliminate this confound in inter-group comparisons. We did not observe a dose-related effect on controllability for most regions in patients with schizophrenia. Nevertheless, we cannot entirely discount the influence of medication. Longitudinal studies preferably in drug-naïve participants are needed for conclusive proof. Because of the limited *n*-back loads used (zero- and two-back), we were not able to study state transitions (controllability) at higher loads. Finally, we lacked in-sample gene expression data from the brain tissue of the same participants who undertook working memory fMRI; gene annotations from public databases may not correspond to the actual regional expression in individual patients.

In conclusion, patients with schizophrenia show lower controllability of multiple brain functional networks during working memory tasks, with these differences intensifying under heightened task load. The differences in modal controllability manifest in the DMN, FPN and salience network, while the differences in average controllability are concentrated in the visual network, auditory network and SMN. Shared regional abnormalities in controllability in siblings and patients occur in regions with higher expression of calmodulin binding and insulin secretion pathway genes; this

effect may arise from shared genetic/environmental influence within families. Our work distinguishes the nature of control signal aberrations in sensory processing versus transmodal regions in working memory deficits in schizophrenia. It also raises the question of the role of insulin signalling, calcium dynamics and more broadly bioenergetic aberrations in the cognitive features of schizophrenia.

**Feiwen Wang** , Department of Psychiatry, and National Clinical Research Center for Mental Disorders, The Second Xiangya Hospital of Central South University, Changsha, China; **Zhening Liu**, Department of Psychiatry, and National Clinical Research Center for Mental Disorders, The Second Xiangya Hospital of Central South University, Changsha, China; **Ju Wang**, Department of Radiology, The Second Xiangya Hospital of Central South University, Changsha, China; **Xiao Li**, Department of Radiology, The Second Xiangya Hospital of Central South University, Changsha, China; **Yunzhi Pan** , Department of Psychiatry, and National Clinical Research Center for Mental Disorders, The Second Xiangya Hospital of Central South University, Changsha, China; **Jun Yang**, Department of Psychiatry, and National Clinical Research Center for Mental Disorders, The Second Xiangya Hospital of Central South University, Changsha, China; **Peng Cheng**, Department of Psychiatry, and National Clinical Research Center for Mental Disorders, The Second Xiangya Hospital of Central South University, Changsha, China; **Fuping Sun**, Department of Psychiatry, and National Clinical Research Center for Mental Disorders, The Second Xiangya Hospital of Central South University, Changsha, China; **Wenjian Tan**, Department of Psychiatry, and National Clinical Research Center for Mental Disorders, The Second Xiangya Hospital of Central South University, Changsha, China; **Danqing Huang**, Department of Psychiatry, and National Clinical Research Center for Mental Disorders, The Second Xiangya Hospital of Central South University, Changsha, China; **Jiamei Zhang**, Department of Psychiatry, and National Clinical Research Center for Mental Disorders, The Second Xiangya Hospital of Central South University, Changsha, China; **Xiawei Liu**, Department of Psychiatry, and National Clinical Research Center for Mental Disorders, The Second Xiangya Hospital of Central South University, Changsha, China; **Maoping Zhong**, Department of Psychiatry, and National Clinical Research Center for Mental Disorders, The Second Xiangya Hospital of Central South University, Changsha, China; **Guowei Wu**, Department of Psychiatry, and National Clinical Research Center for Mental Disorders, The Second Xiangya Hospital of Central South University, Changsha, China; **Jie Yang** , Department of Psychiatry, and National Clinical Research Center for Mental Disorders, The Second Xiangya Hospital of Central South University, Changsha, China; **Lena Palaniyappan** , Douglas Mental Health University Institute, Department of Psychiatry, McGill University, Montreal, Canada; Department of Medical Biophysics, Schulich School of Medicine and Dentistry, Western University, London, Canada; and Robarts Research Institute, Schulich School of Medicine and Dentistry, Western University, London, Canada

**Correspondence:** Jie Yang. Email: yang0826@csu.edu.cn

First received: 22 Apr 2024, revised 17 Sep 2024, accepted 5 Oct 2024

## Supplementary material

Supplementary material is available online at <https://doi.org/10.1192/bjp.2024.225>

## Data availability

Network control theory code can be found at [https://complexsystemsupenn.com/s/controllability\\_code-smb8.zip](https://complexsystemsupenn.com/s/controllability_code-smb8.zip). Other custom analytic codes supporting the findings are available from the corresponding author upon reasonable request. The data supporting the findings are available from the corresponding author upon reasonable request.

## Acknowledgements

We would like to thank all participants in this study.

## Author contributions

Jie Yang, Z.L. and L.P. designed the research. F.W., J.W., X. Li, Y.P., Jun Yang, P.C., F.S., W.T., D.H., J.Z., X. Liu, M.Z. and G.W. collected the data. F.W. and Jie Yang analysed the data and wrote the manuscript along with L.P. Z.L. and L.P. revised various versions of the manuscript. All authors reviewed the manuscript and approved the submitted version.

## Funding

This work was supported by grants from the National Natural Science Foundation of China (82201663 to Jie Yang; 82071506 to Z.L.), the Training Program for Excellent Young Innovators of Changsha (kq2306008 to Jie Yang), the Scientific Research Program of Hunan Provincial Health Commission, China (B202303095947 to Jie Yang) and the Scientific Research Launch Project for new employees of the Second Xiangya Hospital of Central South University to Jie Yang. L.P.'s research is supported by the Canada First Research Excellence Fund, awarded to the Healthy Brains, Healthy Lives initiative at McGill University (through a New Investigator Supplement to L.P.) and Monique H. Bourgeois Chair in Developmental Disorders. He receives a salary award from the Fonds de recherche du Québec-Santé (FROS).

## Declaration of interest

L.P. reports personal fees for serving as chief editor from the Canadian Medical Association Journals, speaker/consultant fee from Janssen Canada and Otsuka Canada, SPMM Course Limited, UK, Canadian Psychiatric Association; book royalties from Oxford University Press; investigator-initiated educational grants from Janssen Canada, Sunovion and Otsuka Canada outside the submitted work. All other authors report no potential conflicts.

## References

- Baddeley A. Working memory. *Science* 1992; **255**(5044): 556–9.
- Agnew-Blais J, Seidman LJ. Neurocognition in youth and young adults under age 30 at familial risk for schizophrenia: a quantitative and qualitative review. *Cogn Neuropsychiatry* 2013; **18**(1–2): 44–82.
- Braff DL, Greenwood TA, Swerdlow NR, Light GA, Schork NJ. Advances in endophenotyping schizophrenia. *World Psychiatry* 2008; **7**(1): 11–8.
- Kringelbach ML, Deco G. Brain states and transitions: insights from computational neuroscience. *Cell Rep* 2020; **32**(10): 108128.
- Menon V, Uddin LQ. Saliency, switching, attention and control: a network model of insula function. *Brain Struct Funct* 2010; **214**(5–6): 655–67.
- Braun U, Schäfer A, Walter H, Erk S, Romanczuk-Seiferth N, Haddad L, et al. Dynamic reconfiguration of frontal brain networks during executive cognition in humans. *Proc Natl Acad Sci U S A* 2015; **112**(37): 11678–83.
- Shine JM, Bissett PG, Bell PT, Koyejo O, Balsters JH, Gorgolewski KJ, et al. The dynamics of functional brain networks: integrated network states during cognitive task performance. *Neuron* 2016; **92**(2): 544–54.
- Yang J, Pu W, Wu G, Chen E, Lee E, Liu Z, et al. Connectomic underpinnings of working memory deficits in schizophrenia: evidence from a replication fMRI study. *Schizophr Bull* 2020; **46**(4): 916–26.
- Braun U, Harneit A, Pergola G, Menara T, Schäfer A, Betzel RF, et al. Brain network dynamics during working memory are modulated by dopamine and diminished in schizophrenia. *Nat Commun* 2021; **12**(1): 3478.
- Wu C, Zheng Y, Li J, Zhang B, Li R, Wu H, et al. Activation and functional connectivity of the left inferior temporal gyrus during visual speech priming in healthy listeners and listeners with schizophrenia. *Front Neurosci* 2017; **11**: 107.
- Braun U, Schäfer A, Bassett DS, Rausch F, Schweiger JI, Bilek E, et al. Dynamic brain network reconfiguration as a potential schizophrenia genetic risk mechanism modulated by NMDA receptor function. *Proc Natl Acad Sci U S A* 2016; **113**(44): 12568–73.
- Li Q, Yao L, You W, Liu J, Deng S, Li B, et al. Controllability of functional brain networks and its clinical significance in first-episode schizophrenia. *Schizophr Bull* 2023; **49**(3): 659–68.
- Gu S, Pasqualetti F, Cieslak M, Telesford QK, Yu AB, Kahn AE, et al. Controllability of structural brain networks. *Nat Commun* 2015; **6**: 8414.
- Jeganathan J, Perry A, Bassett DS, Roberts G, Mitchell PB, Breakspear M. Fronto-limbic dysconnectivity leads to impaired brain network controllability in young people with bipolar disorder and those at high genetic risk. *Neuroimage Clin* 2018; **19**: 71–81.
- Cai W, Ryali S, Pasumarthy R, Talasila V, Menon V. Dynamic causal brain circuits during working memory and their functional controllability. *Nat Commun* 2021; **12**(1): 3314.
- Sun H, Jiang R, Dai W, Dufford AJ, Noble S, Spann MN, et al. Network controllability of structural connectomes in the neonatal brain. *Nat Commun* 2023; **14**(1): 5820.
- Park MTM, Jeon P, French L, Dempster K, Chakravarty MM, MacKinley M, et al. Microstructural imaging and transcriptomics of the basal forebrain in first-episode psychosis. *Transl Psychiatry* 2022; **12**(1): 358.
- Power JD, Cohen AL, Nelson SM, Wig GS, Barnes KA, Church JA, et al. Functional network organization of the human brain. *Neuron* 2011; **72**(4): 665–78.
- Liu Z, Rolls ET, Liu Z, Zhang K, Yang M, Du J, et al. Brain annotation toolbox: exploring the functional and genetic associations of neuroimaging results. *Bioinformatics* 2019; **35**(19): 3771–8.
- Leucht S, Samara M, Heres S, Patel MX, Furukawa T, Cipriani A, et al. Dose equivalents for second-generation antipsychotic drugs: the classical mean dose method. *Schizophr Bull* 2015; **41**(6): 1397–402.
- Guo S, He N, Liu Z, Linli Z, Tao H, Palaniyappan L. Brain-wide functional dysconnectivity in schizophrenia: parsing diathesis, resilience, and the effects of clinical expression. *Can J Psychiatry* 2020; **65**(1): 21–9.
- Mizuno Y, Wiertelsteiner F, Frajo-Apor B. Resilience research in schizophrenia: a review of recent developments. *Curr Opin Psychiatry* 2016; **29**(3): 218–23.
- Xi C, Liu Z, Zeng C, Tan W, Sun F, Yang J, et al. The centrality of working memory networks in differentiating bipolar type I depression from unipolar depression: a task-fMRI study. *Can J Psychiatry* 2023; **68**(1): 22–32.
- Menon V. Large-scale brain networks and psychopathology: a unifying triple network model. *Trends Cogn Sci* 2011; **15**(10): 483–506.
- Niendam TA, Laird AR, Ray KL, Dean YM, Glahn DC, Carter CS. Meta-analytic evidence for a superordinate cognitive control network subserving diverse executive functions. *Cogn Affect Behav Neurosci* 2012; **12**(2): 241–68.
- Pu W, Luo Q, Palaniyappan L, Xue Z, Yao S, Feng J, et al. Failed cooperative, but not competitive, interaction between large-scale brain networks impairs working memory in schizophrenia. *Psychol Med* 2016; **46**(6): 1211–24.
- Luo Q, Pan B, Gu H, Simmonite M, Francis S, Liddle PF, et al. Effective connectivity of the right anterior insula in schizophrenia: the saliency network and task-negative to task-positive transition. *Neuroimage Clin* 2020; **28**: 102377.
- Schlösser R, Gesierich T, Kaufmann B, Vucurevic G, Hunsche S, Gawehn J, et al. Altered effective connectivity during working memory performance in schizophrenia: a study with fMRI and structural equation modeling. *Neuroimage* 2003; **19**(3): 751–63.
- Honey GD, Bullmore ET, Soni W, Varatheesan M, Williams SC, Sharma T. Differences in frontal cortical activation by a working memory task after substitution of risperidone for typical antipsychotic drugs in patients with schizophrenia. *Proc Natl Acad Sci U S A* 1999; **96**(23): 13432–7.
- Fransson P, Schiffler BC, Thompson WH. Brain network segregation and integration during an epoch-related working memory fMRI experiment. *Neuroimage* 2018; **178**: 147–61.
- Pasternak T, Greenlee MW. Working memory in primate sensory systems. *Nat Rev Neurosci* 2005; **6**(2): 97–107.
- Michalka SW, Kong L, Rosen ML, Shinn-Cunningham BG, Somers DC. Short-term memory for space and time flexibly recruit complementary sensory-biased frontal lobe attention networks. *Neuron* 2015; **87**(4): 882–92.
- Zarghami TS, Zeidman P, Razi A, Bahrami F, Hossein-Zadeh GA. Dysconnection and cognition in schizophrenia: a spectral dynamic causal modeling study. *Hum Brain Mapp* 2023; **44**(7): 2873–96.
- Wang F, Xi C, Liu Z, Deng M, Zhang W, Cao H, et al. Load-dependent inverted U-shaped connectivity of the default mode network in schizophrenia during a working-memory task: evidence from a replication functional MRI study. *J Psychiatry Neurosci* 2022; **47**(5): E341–50.
- Borgwardt SJ, Picchioni MM, Ettinger U, Touloupoulou T, Murray R, McGuire PK. Regional gray matter volume in monozygotic twins concordant and discordant for schizophrenia. *Biol Psychiatry* 2010; **67**(10): 956–64.
- Chang M, Womer FY, Bai C, Zhou Q, Wei S, Jiang X, et al. Voxel-based morphometry in individuals at genetic high risk for schizophrenia and patients with schizophrenia during their first episode of psychosis. *PLoS One* 2016; **11**(10): e0163749.
- Han KS, Cooke SF, Xu W. Experience-dependent equilibration of AMPAR-mediated synaptic transmission during the critical period. *Cell Rep* 2017; **18**(4): 892–904.
- Lee SH, Zabolotny JM, Huang H, Lee H, Kim YB. Insulin in the nervous system and the mind: functions in metabolism, memory, and mood. *Mol Metab* 2016; **5**(8): 589–601.
- Arruda AL, Khandaker GM, Morris AP, Smith GD, Huckins LM, Zeggini E. Genomic insights into the comorbidity between type 2 diabetes and schizophrenia. *Schizophrenia (Heidelb)* 2024; **10**(1): 22.
- Dickman DK, Davis GW. The schizophrenia susceptibility gene dysbindin controls synaptic homeostasis. *Science* 2009; **326**(5956): 1127–30.

